Available online at www.sciencedirect.com

SciVerse ScienceDirect

Ceramics International 38 (2012) 2883–2887

CERAMICS INTERNATIONAL

www.elsevier.com/locate/ceramint

Electromagnetic field effects on the formation of MgO dense layer in low carbon MgO–C refractories

Xiangcheng Li *, Boquan Zhu, Tangxi Wang

The State Key Laboratory Cultivation Base of Refractories and Ceramics, Wuhan University of Science and Technology, Wuhan 430081, China

Received 1 November 2011; received in revised form 22 November 2011; accepted 22 November 2011
Available online 29 November 2011

Abstract

Electromagnetic field (EMF) would speed up the corrosion of low carbon MgO–C refractories. Its influence mechanism will be investigated in this paper. The slag-resistance experiments of low carbon MgO–C refractories were carried out under the condition of an induction furnace and a resistance furnace, respectively. Low carbon MgO–C refractories with carbon of 6% (in mass) and a slag with the basicity (CaO/SiO_2) of around 0.87 were used in the experiments. The slag line of MgO–C refractories corroded by the slag under the different conditions were analyzed by X-ray diffractometer (XRD), scanning electron microscope (SEM) and energy dispersive spectrometer (EDS). The results show that in the induction furnace with an electromagnetic field (EMF), no MgO dense layer exists in the interface. However, MgO dense layer could be formed in the interface without any EMF. The formation mechanism of MgO dense layer indicates that the EMF could enhance the solution of MgO and power of Mg (g) discharge. As a result, EMF restrains the formation of MgO dense layer.

Keywords: Refractories; Electromagnetic field; Magnesium oxide–carbon; Dense layer

1. Introduction

MgO–C refractories have been widely used as furnace lining in steelmaking industry and retained an important role in refractories industry. The comprehensive properties such as thermal shock resistance, slag resistance and anti-oxidation for MgO–C refractories have been studied in detail [1,2]. During the application process of the refractories, the formation of MgO dense layer was detected first by Herron et al. [3]. Dense MgO layer has a great effect on slag resistance and anti-oxidation for MgO–C refractories [4,5]. Lee [6] and Fruehan [7] revealed that the formation of MgO dense layer could be easily affected by slag basicity and the purity of raw materials. Guo et al. [8] further pointed out that a fully dense MgO layer cannot be formed under the low oxygen pressure conditions. Boher et al. [9] found that both the composition and thickness of MgO dense layer are related to the chemical composition of the metallic bath, particularly to the oxygen activity. So far, many studies have indicated that the formation of MgO dense layer has arisen from the reduction of MgO by carbon to Mg vapor that is transported to the hot face where it is subsequently re-oxidized by oxygen. And MgO dense layer could be determined by such operating environments as atmosphere, slag basicity and purity of raw materials. However in the literature few papers have been published about the effect of electromagnetic field (EMF) on the formation of MgO dense layer for MgO–C refractories.

Actually, EMF is widely used in steel metallurgy to heat, stir, separate and control flow velocity and shape of molten metal with the uncontact method during the process of long flow rout steelmaking. At the same time, EMF universally exists in the field of arc/induction furnace and secondary refining during the short flow route steelmaking [10,11]. Present researches [12–16] proved EMF can change the wettability of liquid slag–refractories, promote the electron transfer and exchange in the interfacial reaction, affect the generation and distribution of high temperature phase or low melting phase, and accelerate the dissolve of refectories in slag. Therefore in theory, the thermodynamics and kinetics for MgO dense formation will be changed by EMF. The authors have found that EMF plays a key role on the reaction of slag/refractories [14,16,17]. For example, EMF can increase the diffusion coefficient of $Fe^{2+/3+}$

* Corresponding author.
E-mail address: lixiangcheng@wust.edu.cn (X. Li).

0272-8842/$36.00
doi:10.1016/j.ceramint.2011.11.061

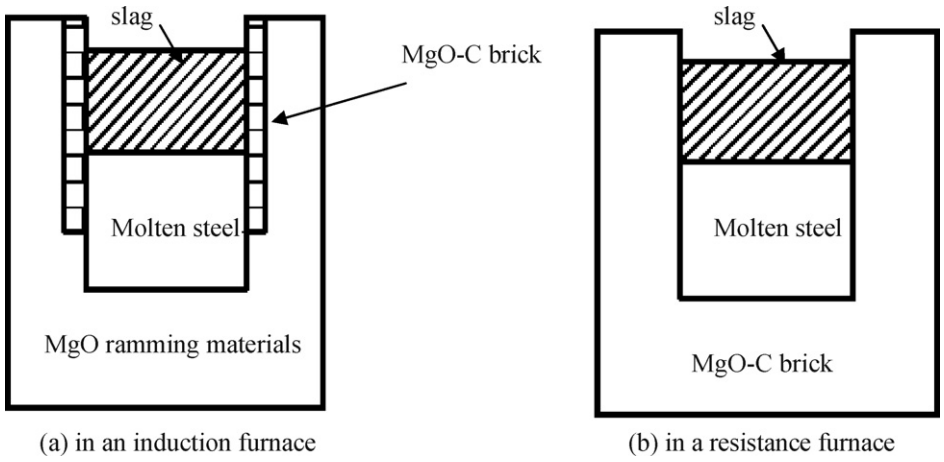

Fig. 1. The schematic diagrams of the experiments.

ions or Mn ion at a high temperature to form $MgFe_2O_4$ with a little of Mn ions. It also would change the penetration kinetics of slag in refractories. But the effect of EMF on the formation of MgO dense layer has not been researched.

The purpose of this paper will reveal the influence mechanism of EMF on the kinetics of dense MgO formation. The slag resistance experiments of MgO–C refractories were carried out under the condition of EMF and EMF-free, respectively. The microstructural change of interfacial layer between slag and MgO–C refractories had been investigated by means of X-ray diffractometer (XRD), scanning electron microscope (SEM) and energy dispersive spectrometer (EDS).

2. Experimental

MgO–C refractories containing 6% carbon and the slag with a basicity (CaO/SiO_2) of around 0.87 were used in the experiments. The chemical composition of the slag is shown in Table 1. MgO–C refractories were dried at 200 °C for 24 h and cut into the cuboid-shaped samples with the dimension of 20 mm × 30 mm × 100 mm. The samples were inserted into the lining of vacuum induction furnace (21WGJL0.025-100-2.5P). Then the steel (6 kg) and slag (2 kg) were filled into the lining. The samples were sintered at 1600 °C × 3 h in Ar with the pressure of 0.1 MPa to carry out the slag resistance experiments under the condition of EMF.

The dried MgO–C refractories were cut into the cube samples with the hole of φ 36 mm × 55 mm. The outer dimension of cube samples was 70 mm × 70 mm × 70 mm. The samples were dried and filled with steel (100 g) and slag (50 g). Then these samples were embedded in carbon and sintered at 1600 °C × 3 h in a resistance furnace. This experiment was the molten slag resistance under the condition of EMF free. The schematic diagrams of the experiments are shown in Fig. 1.

Table 1
Chemical composition of slag (mass%).

Fe_2O_3	SiO_2	Al_2O_3	MnO	MgO	CaO	TiO_2	V_2O_5	C/S
11.34	32.86	10.81	2.15	8.31	28.73	1.84	0.45	0.87

The phase change of slag line for corroded MgO–C refractories was analyzed by means of X-ray diffractometer (XRD, X'Pert pro). The microstructure change was determined by scanning electron microscope (SEM, XL30TMP) and energy dispersive spectrometer (EDS, Pheoenix).

3. Results and discussion

3.1. Effect of EMF on the phase change of corroded MgO–C refractories

Under the condition of EMF and EMF free, the XRD spectra of slag corroded layer for MgO–C refractories are shown in Fig. 2. It reveals that under two conditions, the major phases are magnesia (MgO) and graphite while the new born phases are spinel, metal and motecellite ($CaMgSiO_4$, CMS) or Akermanite ($Ca_2MgSi_2O_7$, C_2MS_2). The difference for two conditions is that in EMF the low melting phase of CMS and metal of Fe exists, while in EMF-free the low melting phase of both CMS and C_2MS_2 can be formed.

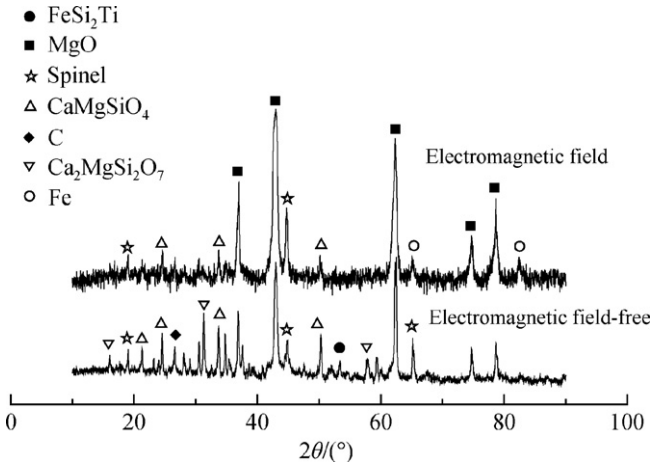

Fig. 2. XRD patterns of slag line for corroded MgO–C refractories under conditions of EMF and EMF-free, respectively.

The SEM of corroded MgO–C refractories in both EMF and EMF free are shown in Fig. 3. Samples A and B indicate the condition of EMF and EMF free respectively. It can be seen in Fig. 3 that samples both A and B have three layers of erosion, penetration and origin. The white region including most metal and slag is the erosion layer (*A*1, *B*1). The gray region including the white region of some metal/slag and black graphite/MgO is the penetration layer (*A*2, *B*2). The black region including MgO and graphite is the original layer (*A*3, *B*3). In EMF, one part of the formed spinel in the interface is $MgAl_2O_4$ (symbol of SP in erosion layer of Fig. 3(a)). The other part is $MgFe_2O_4$ with a little of Mn (symbol of E in Figs. 3 and 4). The low melting phase is CMS shown as symbol of Lm in Fig. 3. While in EMF free, all the spinel is $MgAl_2O_4$ spinel and the low melting phases are CMS and C_2MS_2. The results agree with the report in Refs. [14,16,17].

It is worthy to note that in EMF the phases of pore, graphite, MgO particles morphology and its interface are obvious in the penetration layer. While in EMF-free, there is an obvious dense layer (point *G* in Fig. 3(b)) in the penetration layer. The structure of this area (shown in Fig. 3(c)) is dense, homogenous and particles-free. The EDS spectrum for the penetration layer in both EMF and EMF-free has been shown in Fig. 4. In EMF, the ions of Fe/Mn diffuse into the penetration layer to form new phase of $MgFe_2O_4$ with a little of Mn (denoted as point *E* in

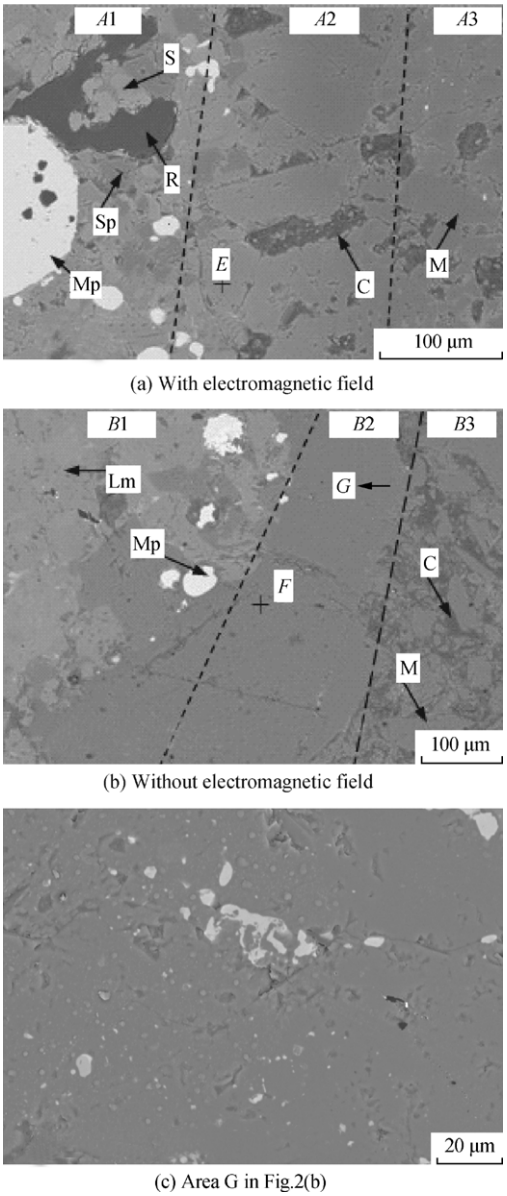

Fig. 3. Scanning electron microscope (SEM) photographs of corroded MgO–C refractories in EMF and EMF-free, respectively. *A*1 and *B*1 represent erosion layer; *A*2 and *B*2 represent penetration layer; *A*3 and *B*3 represent original layer; Lm – low metalling phase; Mp – metal particle; Sp – spinel; R – resin; S – solid solution equal with Lm; M – magnesia; C – graphite; point *E* – one point in *A*2; point *F* – one point in *B*2.

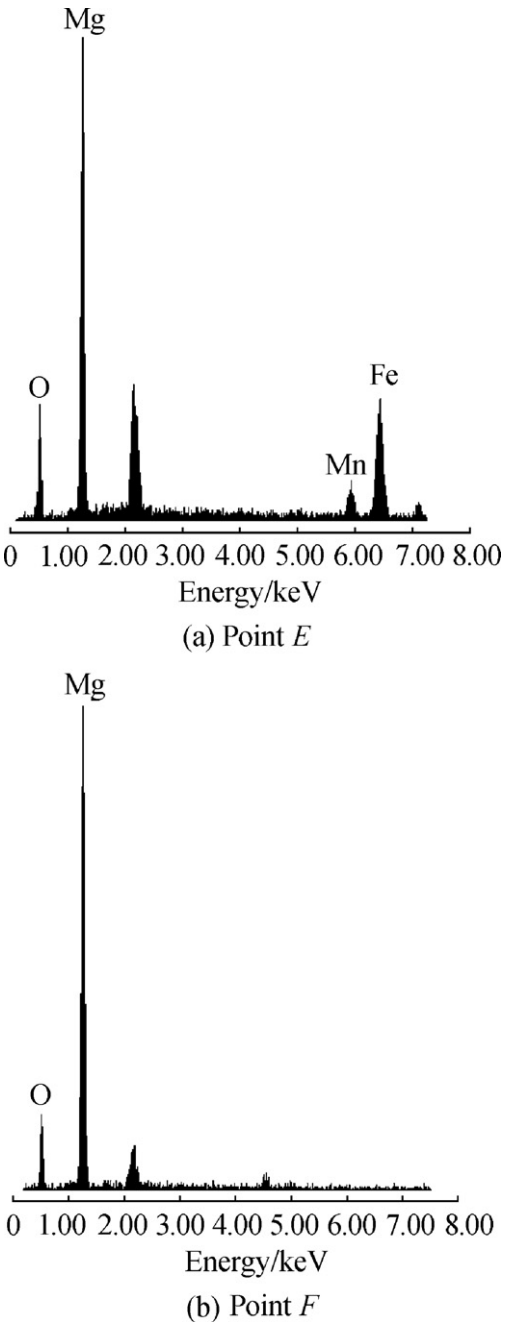

Fig. 4. Energy dispersive spectrometer (EDS) spectra of points *E* and *F* in Fig. 3.

Fig. 4(a)). The dense layer cannot exist. While in EMF free, MgO dense layer has been formed, denoted as point *F* in Fig. 4(b). EMF enhances the substitution of $Fe^{3+/2+}$ and Mn^{2+} in slag for Mg^{2+} in refractories and forms s $MgFe_2O_4$ spinels with a little of Mn [17–19]. In EMF free, reduction of MgO by carbon forms Mg vapors which deoxidizes and deposits as a dense layer of secondary MgO in the penetration layer [6,8].

3.2. Effect of EMF on the formation mechanism of MgO dense layer

In order to further study the above experiments and results, the mechanism of MgO dense layer can be inferred. The formation mechanisms of MgO dense layer can be described in four stages: the generation of Mg vapor, diffusion, reoxidation and recrystallization of MgO [6,8,20–22]. The formation of MgO dense layer could be affected by two factors including the discharge of Mg as a bubble and dissolve of recrystallization for MgO. Mg bubble formation conditions is as follows [20–22]:

$$P_i = P + \frac{2\sigma}{r}$$

where P_i is the partial pressure of Mg bubble, P is the total pressure of bubbles, σ is the surface stress of the slag and r is the radius of bubble. When the Mg bubble could be discharged, MgO dense layer would not be formed.

On the other side, the process of recystallization and solution of MgO could simultaneously happen. Only when the formation rate (J_a) of MgO is larger than its dissolve rate (J_b), can the recrystallization of MgO occur. The kinetic function for the formation and solution of MgO is given by [6,8,20–22]:

$$J_a = KC^n, \qquad J_b = \beta(C_s - C)$$

where K and n are respectively the reaction rate constant and the reaction order. β and C are respectively the mass transfer coefficient and concentration for solutes. Because the concentration (C) and saturation concentration (C_s) are determined in the system of slag and MgO–C refractories, the factors of K and β would play a key influence in the formation and solution for MgO dense layer.

Combined the above theory with the experiments, it could be inferred that EMF enhances the generation of Mn-doped $MgFe_2O_4$ spinels, prevents the reduction of MgO by carbon and leads to the decrease of Mg vapor. At the same time, EMF promotes the wettability and diffusion of slag in MgO–C refractories [13,15,17]. That would enlarge the diffusion channel of Mg vapor from the slag [23] and ultimately decrease the total pressure of Mg bubble. On the other side, the penetration enhancement of the slag in EMF would improve the dissolve of MgO [14,15,17]. That causes the dissolve rate (J_b)

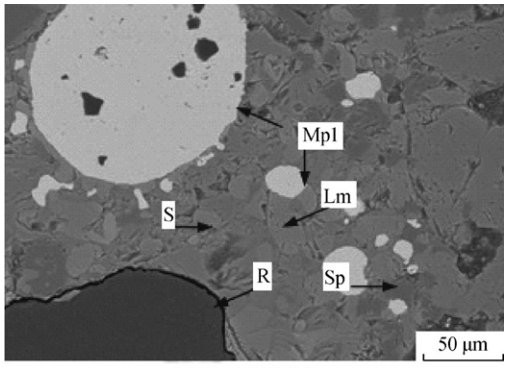

(a) Magnified A1 layer

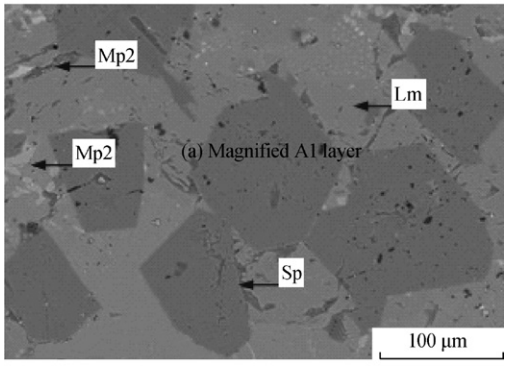

(b) Magnified B1 layer

Fig. 5. Magnified SEM photographs of corroded layers for MgO–C refractories in Fig. 3. Mp1 – Fe particles; Mp2 – Fe-containing particles.

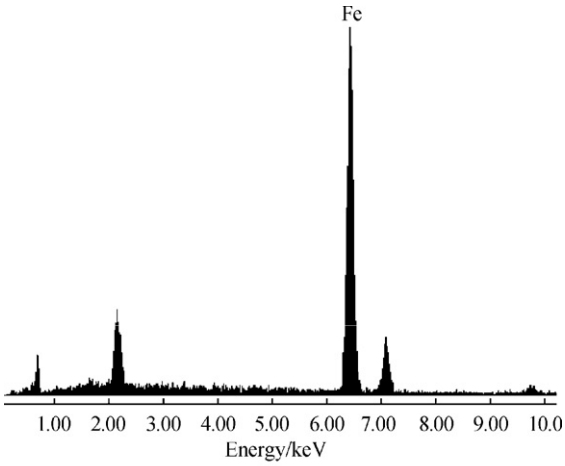

(a) EDS pattern of point Mp1 in Fig.4(a)

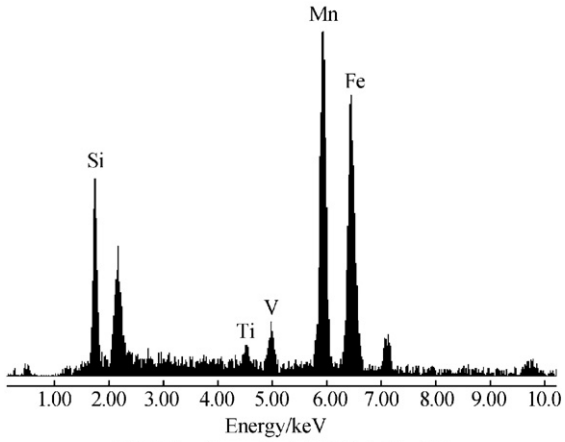

(a) EDS pattern of point Mp2 in Fig.4(b)

Fig. 6. EDS patterns of metal particle in corrosion layers under the condition of EMF and EMF-free.

of MgO to be larger than its formation rate (J_a). As a result, MgO dense layer cannot be formed.

The magnified SEM for layers of *A*1 and *B*1 in Fig. 3 are shown in Fig. 5. The phases in erosion layers in both EMF and EMF-free are low melting phases, high temperature phases and the metal particles. The EDS patterns in Fig. 6 reveal that in EMF the reduced metal is iron (denoted as Mp1 in Fig. 5(a)), while in EMF-free the reduced metal is Fe alloy containing of Mn, Ti, V and Si (denoted as Mp2 in Fig. 5(b)), which distributes in the interface between the erosion layer and the penetration layer. In EMF the high temperature phases are Mn-doped $MgFe_2O_4$ spinel and $MgAl_2O_4$ spinel, shown as points of S and Sp in Fig. 5(a). While in EMF-free the high temperature phase is $MgAl_2O_4$ spinel (Sp in Fig. 5(b)), distributing in the low melting phase.

EMF prevents the formation of MgO dense layer and enhances the corrosion of MgO–C refractories by slag. While in EMF-free, the dense MgO layer formed in the hot face can facilitate the corrosion resistance of MgO–C refractories.

4. Conclusion

(1) In EMF, MgO dense layer cannot be formed in the interface of slag/MgO–C refractories. While in EMF-free, recrystallization and growth of secondary MgO form dense layer, which facilitates the corrosion resistance of MgO–C refractories.
(2) EMF enhances the dissolve rate of MgO, decreases the pressure of Mg vapor bubble and ultimately prevents the formation of MgO dense layer.

Acknowledgment

Authors wish to appreciate the financial support of the National Natural Science Foundation of China (Grant No. 50904048 and Grant No. 51174152).

References

[1] S. Chatterjee, R. Eswaram, Continual improved performance MgO–C refractory for BOF[C], in: 11th Unified International Technical Conference Refractories, Salvador, Brazil, (2009), pp. 136–140.
[2] S. Zhang, N.J. Marriott, W.E. Lee, Thermochemistry and microstructures of MgO–C refractories containing various antioxidants, J. Eur. Ceram. Soc. 21 (2001) 1037–1047.
[3] R.H. Herron, C.R. Beechan, R.C. Padfield, Slag attack on carbon-bearing basic refractories, Am. Ceram. Soc. Bull. 46 (1967) 1163–1168.
[4] B.M. Vandchali, H. Sarpoolaky, F. Fard, et al., Atmosphere and carbon effects on microstructure and phase analysis of *in situ* spinel formation in MgO–C refractories matrix, Int. Ceram. 35 (2009) 861–868.
[5] S. Jansson, V. Brabie, P. Jonsson, Corrosion mechanism of commercial MgO–C refractors in contact with different gas atmospheres, ISIJ Int. 48 (2008) 760–767.
[6] W.E. Lee, S. Zhang, Melt corrosion of oxide and oxide–carbon refractories, Int. Mater. Rev. 44 (1999) 77–104.
[7] R.J. Fruehan, L.J. Martonik, The rate of reduction of MgO by carbon, Met. Trans. B 7B (1976) 537–542.
[8] M. Guo, S. Parada, P.T. Jones, et al., Interaction of Al_2O_3-rich slag with MgO–C refractories during VOD refining—MgO and spinelformation at the slag/refractory interface, J. Eur. Ceram. Soc. 29 (2009) 1053–1060.
[9] M. Boher, J. Lehmann, H. Soulard, et al., Physico-chemical study of reactions between a magnesia–graphite refractory and liquid steel, Key Eng. Mater. 132–136 (1997) 1854–1857.
[10] L.B. Khoroshavin, B. Shcherbatskii, An electronic technology for refractories based in periodic law, Refract. Ind. Ceram. 5 (2005) 344–350.
[11] A. Bermudez, D. Gomez, M. Muniz, C. Numberical, simulation of a thermo-electromagneto-hydrodynamic problem in an induction heating furnace, Appl. Numer. Math. 59 (2009) 2084–2104.
[12] J. Potschke, Does electrowetting influence slag infiltration, in: 51st International Colloquium on Refractories–Refractories for Metallurgy, Eurogress Aachen, Germany, 2008, pp. 144–146.
[13] C.G. Aneziris, M. Hampel, Microstructured and electro-assisted high temperature wettability of MgO in contact with a silicate slag based on fayalite, Int. J. Appl. Ceram. Technol. 5 (2008) 469–479.
[14] X.C. Li, T.X. Wang, B.Q. Zhu, Effect of electromagnetic field on the slag resistance of MgO–C refractories, in: IOP Conf. Ser. Mater. Sci. Eng., vol. 18, 2011, p. 222003.
[15] C.G. Aneziris, F. Homola, Electrical assisted high temperature wettability in oxide and carbon based refractories, Interceram. Refract. Annu. 31 (2004) 52–56.
[16] X.C. Li, T.X. Wang, B.Q. Zhu, X. Jiang, P. Xu, Effect of electromagnetic field on melting slag resistance of MgO–C refractories, J. Chin. Ceram. Soc. 39 (2011) 452–457.
[17] X.C. Li, B.Q. Zhu, T.X. Wang, Effect of electromagnetic field on slag corrosion resistance of low carbon MgO–C refractories, Ceram. Int., doi:10.1016/j.ceramint.2011.10.049.
[18] O. Lioubashevski, E. Katz, I. Wilner, Magnetic field effects on electrochemical processes: a theoretical hydrodynamic model, J. Phys. Chem. B 108 (2004) 5778–5784.
[19] J.M.D. Coey, G. Hinds, Magnetic electrodeposition, J. Alloys Compd. 326 (2001) 238–245.
[20] S.M. Kim, W.K. Lu, Kinetics and mechanism of the formation of dense MgO layer in pitch bearing magnesite brick during service, Met. Trans. B (9B) (1978) 353–364.
[21] P. Vincenzini, Effect of dense layer formation on dissolution rate of MgO–C refractory in molten slag, Adv. Sci. Tech. 45 (2006) 162–166.
[22] M. Kohno, T. Matsui, H. Minamizona, et al., Microstructure and formation of dense MgO layer in MgO–C refractory, Tech. Assoc. Refract. Jpn. 56 (2004) 146.
[23] Q.Z. Shi, Y.C. Liu, G.Z. Gao, Formation of MgO whiskers on the surface of bulk MgB_2 superconductors during *in situ* sintering, J. Mater. Sci. 43 (2008) 1438–1443.